SSC-139

SSC-139

ON EFFECTS OF CARBON AND MANGANESE CONTENT AND OF GRAIN SIZE ON DYNAMIC STRENGTH PROPERTIES OF MILD STEEL

by

J. M. Krafft

and

A. M. Sullivan

SHIP STRUCTURE COMMITTEE

SHIP STRUCTURE COMMITTEE

MEMBER AGENCIES:

BUREAU OF SHIPS, DEPT. OF NAVY
MILITARY SEA TRANSPORTATION SERVICE, DEPT. OF NAVY
UNITED STATES COAST GUARD, TREASURY DEPT.
MARITIME ADMINISTRATION, DEPT. OF COMMERCE
AMERICAN BUREAU OF SHIPPING

ADDRESS CORRESPONDENCE TO:

SECRETARY
SHIP STRUCTURE COMMITTEE
U. S. COAST GUARD HEADQUARTERS
WASHINGTON 25, D. C.

December 27, 1961

Dear Sir:

As part of its research program related to the improvement of hull structures of ships, the Ship Structure Committee is sponsoring an investigation at the Naval Research Laboratory to determine what occurs when steel is stressed at a high strain rate, and how this may relate to brittle fracture.

Herewith is a copy of the final report of this investigation, Serial No. SSC-139, entitled On Effects of Carbon and Manganese Content and of Grain Size on Dynamic Strength Properties of Mild Steel by J. M. Krafft and A. M. Sullivan.

The project is being conducted under the advisory guidance of the Committee on Ship Steel of the National Academy of Sciences-National Research Council.

Please address any comments concerning this report to the Secretary, Ship Structure Committee.

Yours sincerely,

J. A. Alger, Jr.
Rear Admiral, U. S. Coast Guard
Chairman, Ship Structure Committee

Serial No. SSC-139

Final Report
of
Project SR-142

to the

SHIP STRUCTURE COMMITTEE

ON EFFECTS OF CARBON AND MANGANESE CONTENT AND OF GRAIN SIZE ON DYNAMIC STRENGTH PROPERTIES OF MILD STEEL

by

J. M. Krafft and A. M. Sullivan

U. S. Naval Research Laboratory
Washington, D. C.

under

Bureau of Ships
Department of the Navy
Index No. NS-011-078

transmitted through

Committee on Ship Steel
Division of Engineering and Industrial Research
National Academy of Sciences-National Research Council

under

Department of the Navy
Bureau of Ships Contract NObs-84321
Index No. S-R 009 03 01 Task 2004

Washington, D. C.
National Academy of Sciences-National Research Council
December 27, 1961

ABSTRACT

The exceptionally low ductility of mild steel when separated by a rapidly moving crack may be attributed in part to its plastic flow strain-rate sensitivity. The elevation in yield strength under conditions of rapidly rising stress adjacent to the crack tip suppresses formation of the energy-absorbing plastic zone. Variation in composition, particularly of carbon and manganese content which affect the notched bar impact transition temperature, should also affect strain-rate sensitivity if this description is applicable. To test this proposition materials, with these elements and grain size varied, were subjected to rapid uniaxial compression. Both impact and a free-piston gunpowder-pressurized machine were used to obtain dynamic stress-strain curves at room temperature. The general trends in yield point strain-rate sensitivity are found in agreement with effects of composition on the Charpy transition temperature. A good correlation is found to exist between the parameter k, found from the grain size dependency of dynamic upper yield strength, and the transition temperature expectancy for given composition. Plastic flow stress, at given high strain rate, can be correlated with free path in ferrite better than with ferrite grain size.

CONTENTS

SR-142 PROJECT ADVISORY COMMITTEE

"Strain Rate and Fracture"

for the

COMMITTEE ON SHIP STEEL

Chairman:

J. R. Low, Jr.
Metallurgy Research Unit
Research Laboratory, General Electric Company

Members:

C. S. Barrett
Institute for the Study of Metals
University of Chicago

J. H. Bechtold
Manager, Metallurgy Department
Westinghouse Research Laboratories, Churchill Boro

L. S. Darken
Assistant Director, Fundamental Research Laboratory
U. S. Steel Corporation

Maxwell Gensamer
Professor of Metallurgy
School of Mines
Columbia University

INTRODUCTION

An understanding of the basic processes of fracture has been the long term objective of this study of flow properties in metals at high rates of strain. During fracture, the energy required for separation is almost totally utilized in the plastic deformation of a volume of material immediately adjacent to the fracture path. This deformed zone, in turn, resists fracture propagation so the two are seen to be closely interrelated. Many fractures become catastrophic only after the crack begins to run rapidly. Any plastic deformation associated with it must also be rapid. To understand and describe the high speed fracture process, the plastic flow properties at high rates of strain must be considered, when these differ from the so-called static properties.

This reasoning supports the experimental evidence that material toughness decreases when high strain rate conditions increase yield and flow strength. Correlation of the static and dynamic flow properties of a mild steel reported by Manjoine[1] with the absorbed energy values of both slow notch bend and Charpy impact tests from the work of Mailander[2] is pertinent. Comparing the slow speed tests it seems plausible to associate the decrease in fracture energy at temperatures below 0°C with the corresponding increase in flow strength. At the strain aging temperature, again fracture energy drops and may be associated with the rise in flow strength. Under dynamic conditions of loading where flow stress elevation occurs at higher temperatures, the Charpy energy minima shift correspondingly.

In reality a spectrum of strain levels is included in the crack environment and should influence the energy used in plastic flow. At low temperatures, for example, the upper or delayed yield strength is markedly greater than the flow strength and markedly more sensitive to strain rate as well. In this region the upper yield strength, rather than the flow stress, may largely control the extent of plastic deformation and thus account for the relatively marked drop in Charpy energy. The work of Hall et al[3] has shown that in mild steel plates recoverable strains adjacent to a rapidly running crack are found which are several times the static yield strain values. There can be little doubt that the yield strength elevation, which is clearly a measure of the delayed yield effect, operates to permit such stress levels to exist without plastic flow. Diminution of the size of the crack-tip-associated plastic zone as a consequence of the increased elastic constraint is reasonably associated with the brittleness of this material.

Models for fracturing of ductile materials have always included some influence of yield and/or flow properties. Ludwig's hypothesis of a yield or flow stress, reaching a "fracture stress" as a condition for crack growth is of historical interest.[4] This analogy, though possibly of use for very ductile fracture of materials possessing no distinct flaws or cracks, is not too helpful in describing brittle fracture. In the fracture mechanics developed by Irwin[5] resistance to crack growth or fracture toughness is expressed in terms of crack stress-field intensity required to propagate the crack. Not unlike the Ludwig hypothesis, this fracture strength parameter is compared to a tensile strength parameter as a measure of brittleness. Thus a crack-tip-associated plastic zone is successfully dimensioned as a function of the ratio of this stress intensity parameter for unstable fracture to the yield stress. This characterization of plastic zone size is necessarily somewhat arbitrary as experimental measures of any fracture toughness parameter inherently reflect the energy contribution of the plastic zone. Toughness measured for conditions of maximum elastic constraint, such as in thick sections of material, should be most suitable.

There are notable cases for which fracture toughness can be reduced essentially independently of the yield strength. Marked reduction in crack-tip-associated plastic deformation is then observed. In fracture of a sheet or plate the extent of the shear lip is a qualitative index of the plastic flow associated with the crack.[6] A subnormal size of this lip is strikingly evident in cases in which the fracture toughness is reduced. Fatigue cracks, where because of localized plastic upset the crack grows with very low crack extension force or applied stress, are characterized by the negligible plastic flow that accompanies them.[7] When the requirement for crack extension force is reduced by chemical action such as stress corrosion effects, abnormally small shear lips are observed.[8] A most striking instance of this effect is seen when damaging salts, such as those of mercury on aluminum, are applied to a crack.[9] Heavy plates of ordinarily tough material can then be broken by hand after which practically no trace of shear lip is seen on the fracture surface, even though without the salts the shear lip would cover the specimen thickness.

If yield stress increases without change in fracture toughness, as might be the case in going to high crack speeds in a rate sensitive material, then the plastic zone size and its energy absorption must decrease. This effect is thought to characterize rapid fracture brittleness of mild steel since this material has long been noted for high strain-rate sensitivity. The role of this sensitivity in the fracture process has been evaluated by studying the effect of reduced temperature on plastic flow properties and then assuming an equivalence between reduced temperature and increased strain rate. A more direct approach is followed in this paper where, at a given temperature, the loading and strain rate are varied to provide direct measure of strain-rate sensitivity. The modification of this sensitivity with changes in manganese content and grain size permits correlation with Charpy notched bar impact test properties of similar materials.

SPECIMEN MATERIAL AND SIZE

The tests were intended to include combinations of three levels of carbon content (roughly 0.1, 0.2 and 0.3%) and three of manganese (0.3, 0.6 and 1.0%). Particulars of this set, with the exception of unavailable

TABLE I

COMPOSITION AND MICROSTRUCTURAL PARAMETERS

Material Heat Treatment, °C	Microstructure	Microstructural Parameters α_1	α_2	β	$d^{-1/2}$
		(10^{-3} mm.)			
1010-2					
(.09 C, 114 Mn, .04 Si)					
FC 870	Non Uniform	21	248	7.6	5.38
1050		74	291	27	2.86
1250	Wid.*	66	284	23	3.04
AC 870	Non Uniform Sub-Str.	34(27)**	142	8.0	4.23
1050		32	137	9.8	4.36
1250	Wid.	41(21)**	122	8.0	3.85
1010-1					
(.11 C, .62 Mn, .23 Si)					
FC 870		14	115	5.4	6.58
1050	Banding Segreg.	30	135	14	4.50
1250		84	295	50	2.58
AC 1050		19	62	7.0	5.65
1250	Wid.	30	87	9.2	4.50
1010-4					
(.12 C, .95 Mn, .06 Si)					
FC 870		8.5	40	7.3	8.55
1050		36	90	22	4.11
1150		53	119	33	3.38
1250		64	165	36	3.08
AC 870	Sub-Str. Segreg.	9.2	39	43	8.23
Project E					
(.22 C, .36 Mn, .002 Si)					
FC 900	Banded	21.1	66	14	5.4
950	"	22	70	15	5.2
1050	"	49	102	34	3.5
1150		54	121	38	3.3
1250		61	123	44	3.1

*Widmanstatten Structure
**Photomicrograph Value

TABLE I (Continued)

Material Heat Treatment, °C	Miscrostructure	α_1	α_2	β	$d^{-1/2}$
		(10^{-3} mm.)			
AC 900		9.9	20	6.7	7.8
1250	Wid.	10.4	15	15	7.6
ABS-B					
(.16 C, .69 Mn, .022 Si)					
FC 900	Banded	36	115	22	4.1
1250		67	194	40	3.1
AC 900	Wid.	13.6	31	5.4	6.7
1250	Wid.	14.3	27	5.4	6.5
EM-3					
(.20 C, 1.12 Mn, .31 Si)					
FC 870	Segreg.	7.7	22	7.7	8.88
1050		29	54	23	4.58
1150		47	80	48	3.59
1250	Acicular Ferrite	53	113	65	3.38
AC 870		7.1	14	4.3	9.25
Mn-1					
(.27 C, .30 Mn, .31 Si)					
FC 870		15	32	11	6.36
1050		31	49	27	4.42
1150		37	63	34	4.05
1250		53	100	55	3.38
AC 900		8.8	17	6.6	8.30
C-5					
(.31 C, 1.01 Mn, .30 Si)					
FC 870		9.2	23	13	8.13
1050		29	37	35	4.57
1250		42	60	52	3.80
AC 1050		8.1	13	9.1	8.66
1250		14	17	29	6.59

medium manganese at high carbon, are given in Table I. Variation in grain size was obtained by heating in the range 900 to 1250 C for one hour followed by slow cooling in the furnace. A somewhat finer grain size was obtained on one set of specimens for each steel by air cooling from 900 C. A few of the materials were also air cooled from 1250 C but at this temperature Widmanstatten structure became a prominent feature to obscure the comparative value of the microstructural size measurements.

Incomplete confidence in any one of the several commonly used measuring methods for grain size parameter led to an attempt to compare results by three methods: (1) by lineal analysis in a Hurlburt-type counter; (2) by linear traverse in three orientations on a photomicrograph; and (3) by chart comparison in a metallograph. The values from the lineal intercept method are recorded in Table I. In most cases agreement among the methods was quite satisfactory. Where differences were large a preference could be established by plotting all three against a particular strength parameter to determine whether the span of values could encompass a simple curve defining a plausible relationship. Recourse to this alternative was necessary for the low carbon low manganese steel (1010-2).

To characterize this pearlitic steel, three parameters were measured: 1) the ferrite linear intercept α_1, taken as the average traverse between ferrite grain boundaries; 2) the ferrite mean free path α_2, the traverse in ferrite between pearlite patches; and 3) the pearlite linear intercept β, the traverse in pearlite between ferrite grains. Grain size is taken as $1.6\alpha_1$, a relationship consistant with that used by Owen et al[10] in measurements on the ABS-B and Project E steels which are reported here for these materials. A consistent interrelationship between size parameters persists throughout for the various heat treatments. A relative increase in pearlite colony size and volume with increasing manganese content is quite evident at all levels of grain size if correction is made for incidental variation in carbon content at a given level.

Unlike the tensile test specimen, permissible length of a compressive specimen is limited by the buckling tendency for large length-to-diameter ratio. On the other hand very short specimens are affected by radial constraint of the ends and by interference of these with diagonal planes of maximum shear stress. The present compressive specimens approach the shorter limitation; most of the data are collected on cylinders 1/2 in. long, 1/2 in. in diameter. Recent work of Ripperger[11] on lead and copper has shown marked increase in apparent yield strength for specimens shorter than this (i.e. L/R = 2) and some decrease for longer specimens. Dynamic tests of longer specimens (L/R = 3.70) of this group have shown a tendency for the upper or delayed yield to be reduced although the effect appears less pronounced than found in lead and copper by Ripperger. In general plastic flow, however, there appears to be essentially negligible difference. Corroborative of the latter in the dynamic tests are a series of static compressive and tensile tests on the 1010-1 steel in 900 C furnace cooled condition (Table II).

TABLE II

STATIC STRESS-STRAIN DATA SHOWING INFLUENCE OF SPECIMEN LENGTH

Material - 1010-1 - Norm. and FC 900 C. Strain measured by head displacement in compressive tests; by extensometer in 0.505-in. tensile.

Test #	OD	Length (in.)	L/R	T or C	$\bar{\bar{\sigma}}_f$ at 4% ϵ 10^3 psi	n
2824	0.5	0.50	2	C	48.0	0.332
2825	0.5	0.50	2	C	47.5	0.33
2807	0.5	0.75	3	C	46.2	0.338
2809	0.5	1.00	4	C	46.0	0.340
2810	0.5	1.50	6	C	45.8	0.328
2811	0.5	1.50	6	C	46.5	0.320
2826	0.505	2.5	10	T	45.8	0.292
2827	0.505	2.5	10	T	47.1	0.295

Here only slight decrease in the flow stress at 4% true strain and in the strain hardening rate (exponent n) are noted. That the tensile specimen should show appreciably lower n (about 13%) is in the direction expected for the reduction of end constraint effects. In view of these results, comparative values of the yield and flow strength measurements on compressive specimens of the same L/R ratio would seem assured. There is good indication that absolute values of these strength parameters would not vary markedly with larger L/R ratio.

TEST APPARATUS AND METHODS

Although bar impact methods provide the highest permissible loading and strain rates, only a limited speed range is available. To increase range at the lower speed end, a gas-pressure actuated loader was employed. Since both machines and data reduction procedures have been analyzed in some detail elsewhere[12] only a brief description will be provided here.

Intermediate Speed Gas Driven Testing Machine

Illustrated in Fig. 1 is the gas driven machine as well as typical oscillograms of load and head displacement versus time and versus each other. Briefly, a pressure source is provided by burning a selected charge of rifle powder in a primed case. The case is chambered within a breech block with its open end abutting an orifice hole. The breech block is threaded into one end of a thick walled steel case which serves as a cylinder for the piston and a rigid loading frame for the specimen. The piston, 1.5 in. in diameter, abuts the breech block at the start of the test and is forced away by the gas entering from the orifice. The load is weighed with wire resistance strain gages applied longitudinally to a short, hard-steel anvil rod which is interposed between piston and specimen. For compression tests, illustrated in Fig. 1, the specimen extends the sectional form of the weighing anvil (1/2-in. diameter circle) and is fixed at the other end by a base which is threaded into the loading frame cylinder.

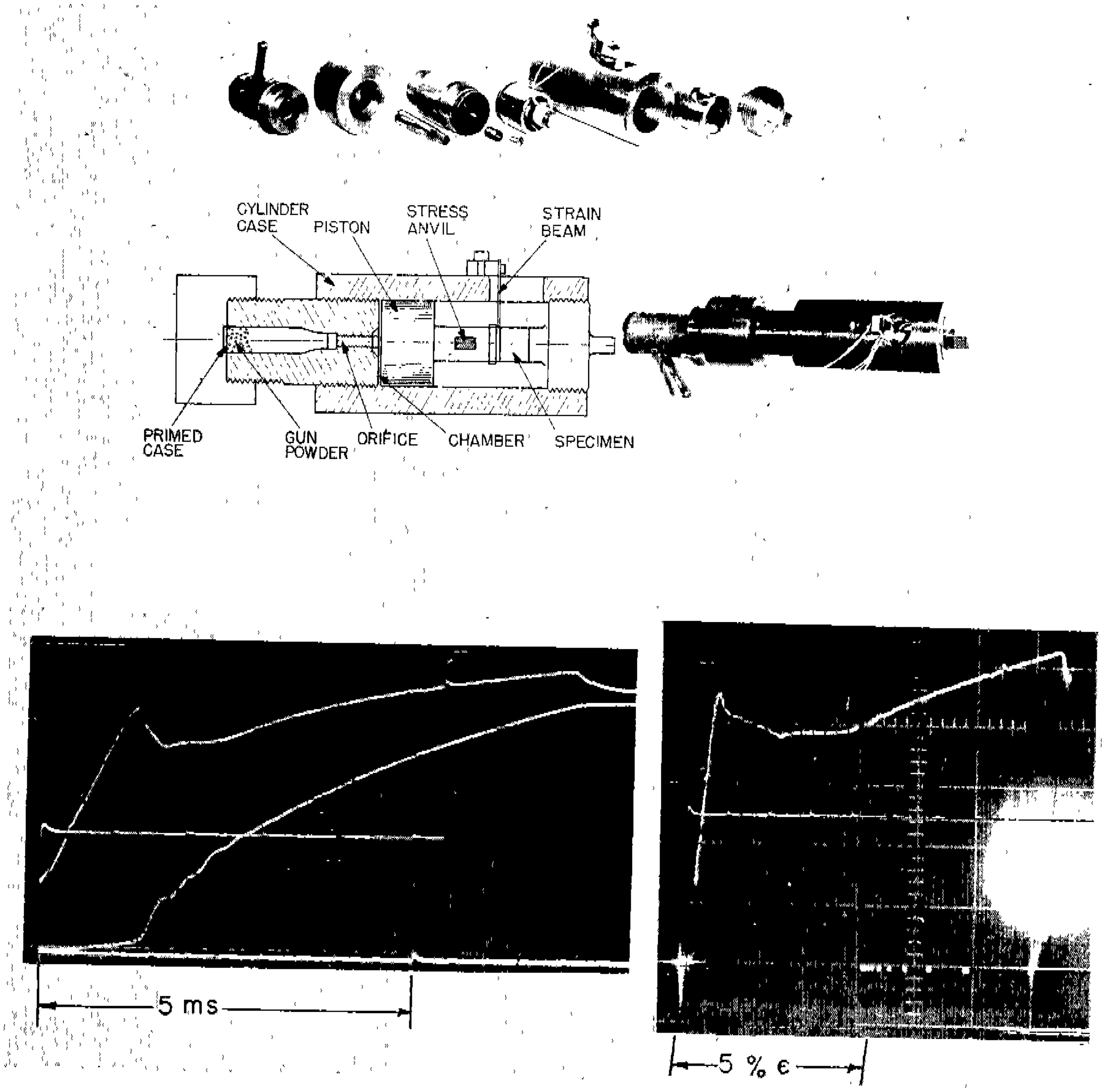

Fig. 1 - Photograph and diagram of and records of load and head displacement for the gas gunpowder pressurized loader. Records at left show variables recorded independently on a common time base while at right, variables with respect to each other have superimposed timing marks.

Motion of the specimen end adjacent to the stress weighing anvil, or the machine head, is followed by the deflection of a strain-gage instrumented tapered cantilever beam fixed in the loading frame at one end and abutting a slight collar near the end of the stress anvil at the other. Strain signals representative of head displacement along with those indicative of load on the weighing anvil are recorded on suitable cathode-ray oscillograph equipment. One mode of recording illustrated in the left-hand portion of Fig. 1 utilizes the

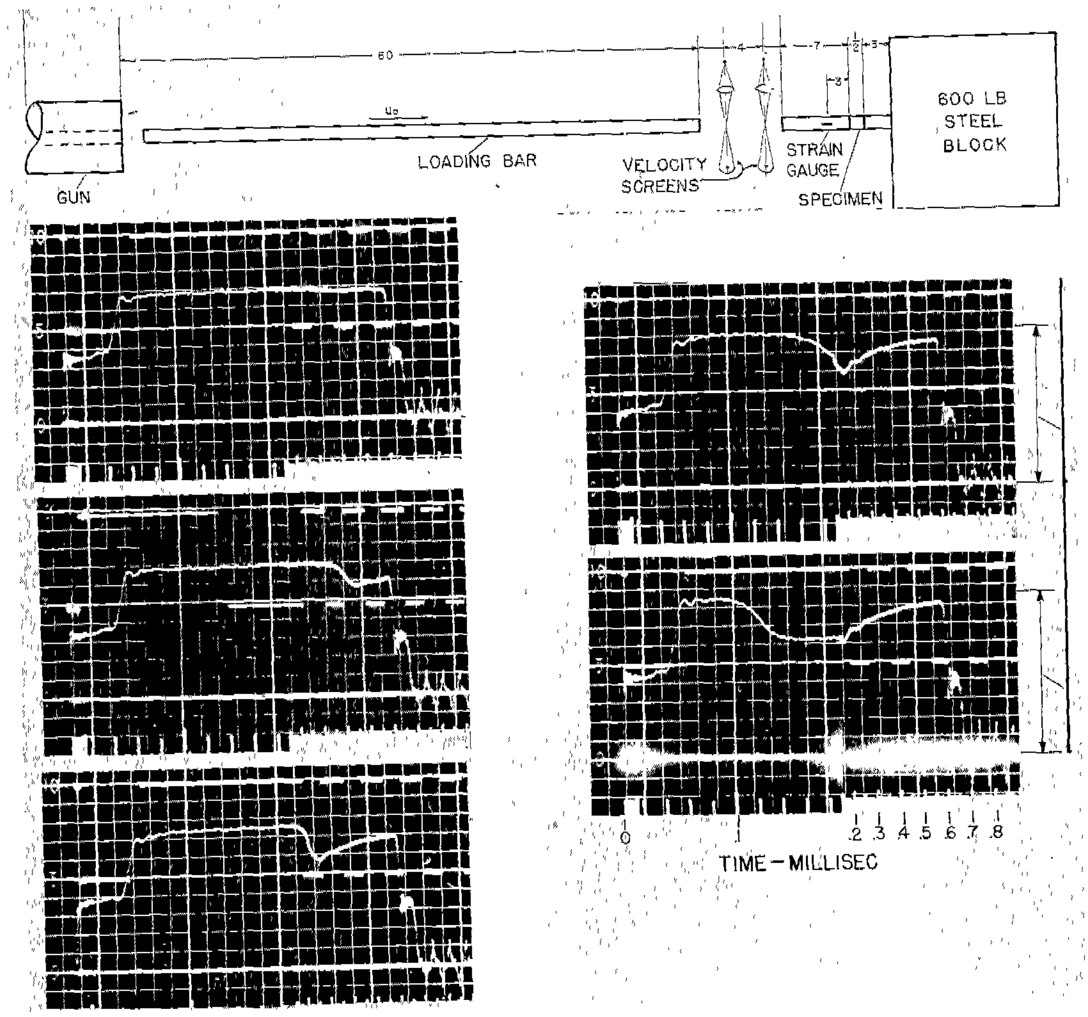

Fig. 2 - Schematic diagram and typical records of bar impact loader. Note expanded scale at beginning of load cycle.

simultaneous dual traces: stress is recorded on the upper trace, strain on the lower one. The other recording technique with stress on one axis, strain on the other of an X-Y oscilloscope is shown in the right-hand portion.

Bar Impact Testing Machine

For low strain levels in mild steel, a head speed of the order of 500 in./sec is generally permissible without involvement in plastic wave phenomena.[13] Gas-pressure driven machines, as typified by the gunpowder-pressurized machine described, are not generally capable of accurate displacement measurement of head speeds in excess of 100 in./sec. The impact bar (Fig. 2) provides a solution to this problem; it permits measurement not only of yield delay but also of stress during post-yield flow as a function of time, strain, and strain rate. Basically the bar impact system is powered by a free, initially unstressed bar of length ℓ_B = 60 in., and is accelerated to a constant longitudinal velocity v_o. If this initial velocity is reduced to zero, as by collision with a rigid "infinite-mass" anvil, a strain wave of amplitude v_o/c is introduced that travels away from the impact surface with elastic bar-wave velocity c. The pressure corresponding to the strain wave amplitude remains on the impact surface until a wave of unloading returns from the opposite end at time $2\ \ell_B/c$ after impact.

To use this constant pressure, a specimen of bar diameter (1/2 in.) is interposed between the colliding bar and the anvil mass. While the specimen remains elastic, a loading stress predictable from the striking velocity is applied. When the specimen yields, the bar-front velocity increases from zero to that allowed by the plastic compression of the specimen. The rate of convergence between bar and anvil— or average strain rate in the specimen—is directly proportional to the amount by which the stress predicted from the striking velocity is reduced. This stress can be measured with wire strain gages on an elastic bar adjacent to the specimen. A single stress-time measurement thus provides a measure of both stress- and strain-rate versus time. With numerical integration to obtain the strain, a stress-strain relationship at rather high strain rates is available to extend the data available with the gas-actuated machine.

PRESENTATION OF BASIC DATA

In static stress-strain curves of mild steel, although either upper or lower yield stress can be used as a measure of strength, the lower is the more reliable. The converse is true of the dynamic test. Here the lower yield is characterized by neither constant stress nor constant strain. Moreover, it represents a combination of effects of rate sensitivities of both the upper yield and of general plastic flow, sensitivities which are of different value and apparently not simply related.[14] Consequently, dynamic yield initiation is best characterized by the upper yield point.

The differing loading patterns inherent in the two types of machines prior to yield initiation require a basis for comparison. In the gas loader, a linearly increasing load (with time) is provided by a roughly constant flow of gas through the restrictive orifice. On the other hand the bar impact provides a suddenly applied constant pressure prior to yield. Comparison of data in the form of a yield stress vs. loading rate with yield stress vs. delay time is possible with the cumulative damage-type criterion suggested in an earlier paper.[15] This involves an assumption that damage culminating in establishment of gross yield accrues at a rate inversely proportional to the delay time (for given stress level). With experimentally determined delay time, the yield point can be predicted for various high loading rates. For the data presented here this has been done for elastic loading rates (i.e. $d\sigma/dt/E$) of 2 and 20/sec. These rates appropriately result in accrual of the gross part of the "damage" at stress levels for which experimental data are available; that is, in the delay time range 10-600 microsec. Characterizing the yield strength elevation in terms of stress rate rather than delay time is preferred here as representing more closely the realistic condition of rising stress in the vicinity of an advancing crack. The stress is not instantly applied to material as it is approached by a rapidly advancing crack tip, but rises rapidly at a roughly uniform rate.

The two measures of yield initiation rate sensitivity are presented for each steel composition in separate graphs. The delay time for constant stress applied with the pressure bar is designated (a) in Figs. 3—10. The yield stress as a function of elastic strain rate prior to yield is designated (b); these curves are extended by the yield strength values predicted from the delay time data (i.e. curve (a) at elastic loading rates of 2 and 20/sec). All grain sizes resulting from the various heat treatments are represented on a single plot for a given composition.

Plastic flow properties are characterized in two ways. Data from the

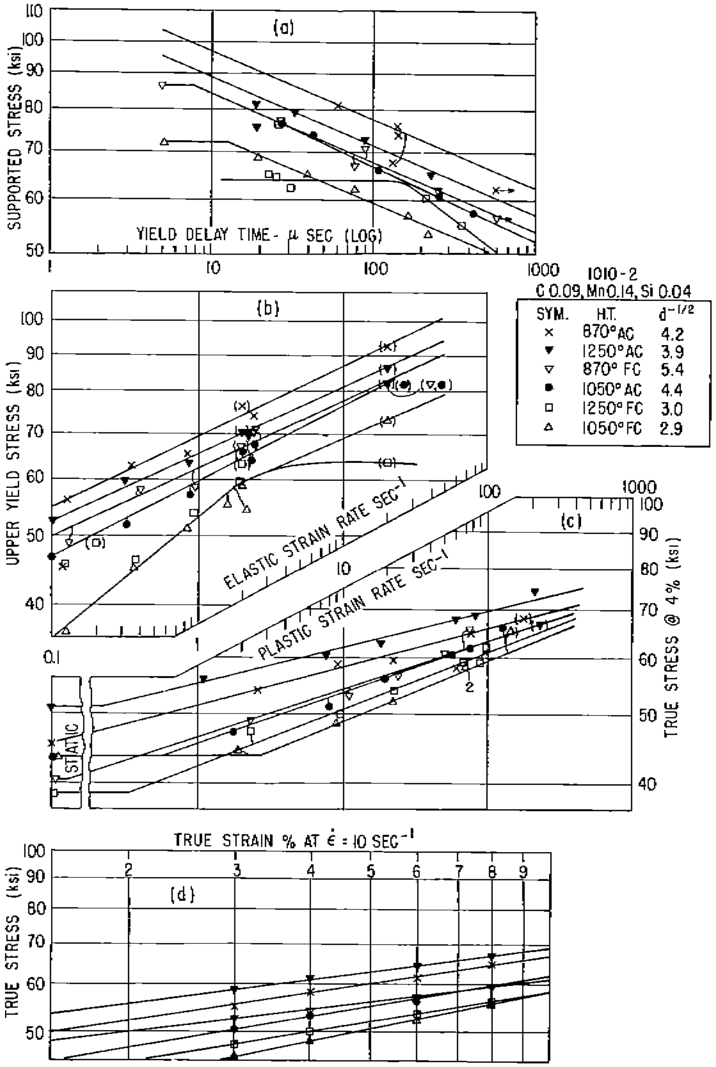

Fig. 3. Summary of dynamic yield and flow data for low carbon, low manganese steel, 1010-2.

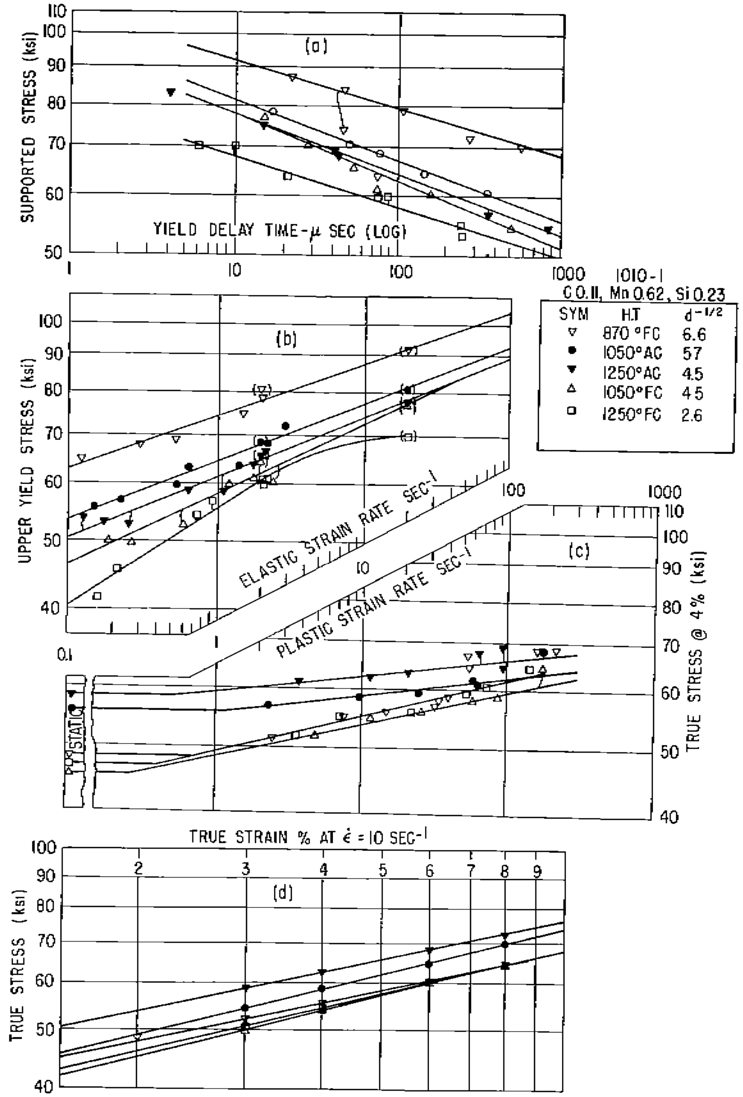

Fig. 4. Summary of dynamic yield and flow data for low carbon, medium manganese steel, 1010-1.

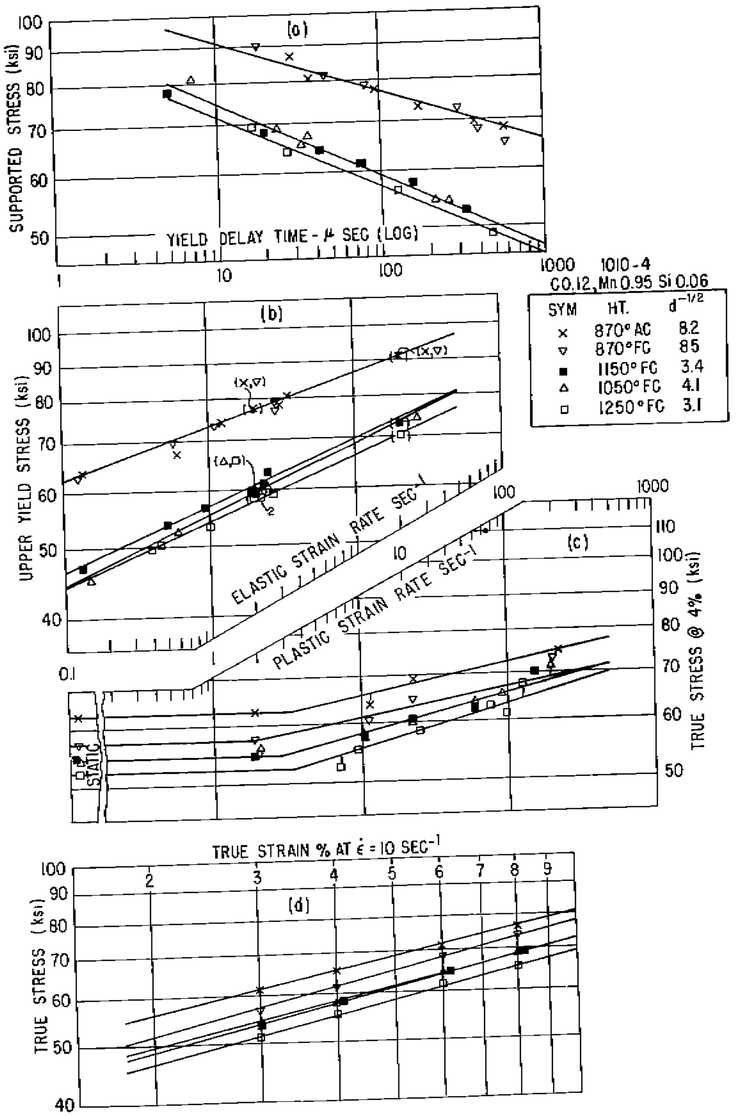

Fig. 5. Summary of dynamic yield and flow data for low carbon, high manganese steel, 1010-4.

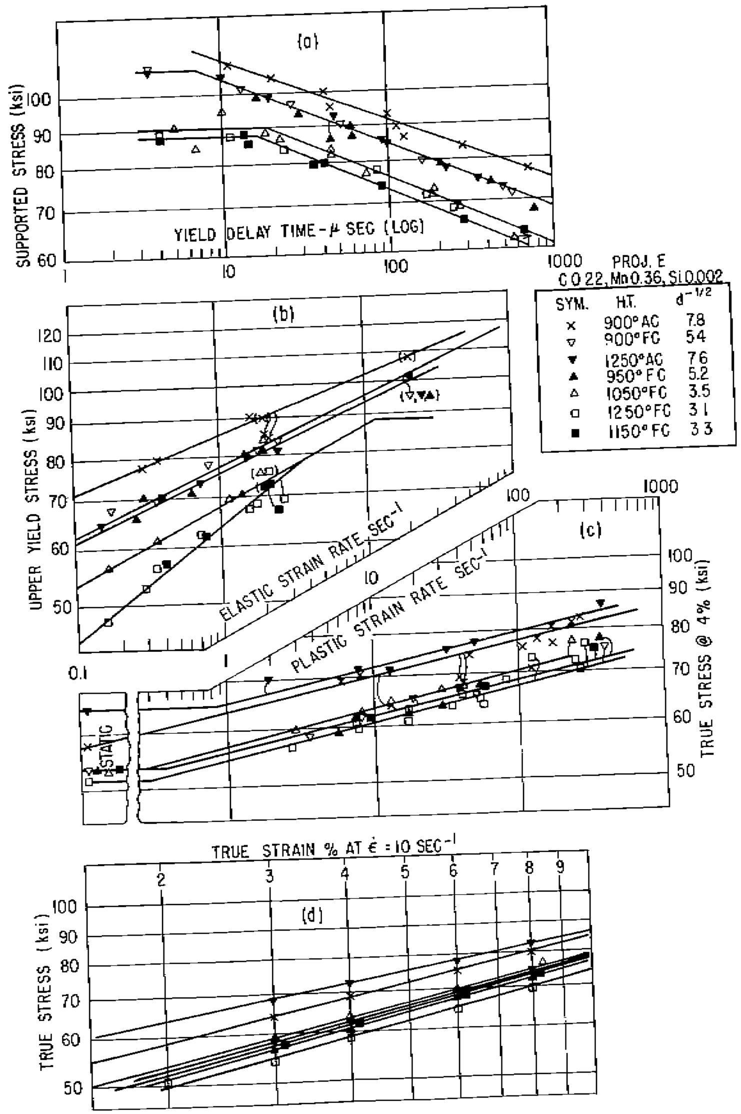

Fig. 6. Summary of dynamic yield and flow data for medium carbon, low manganese steel, Proj. E.

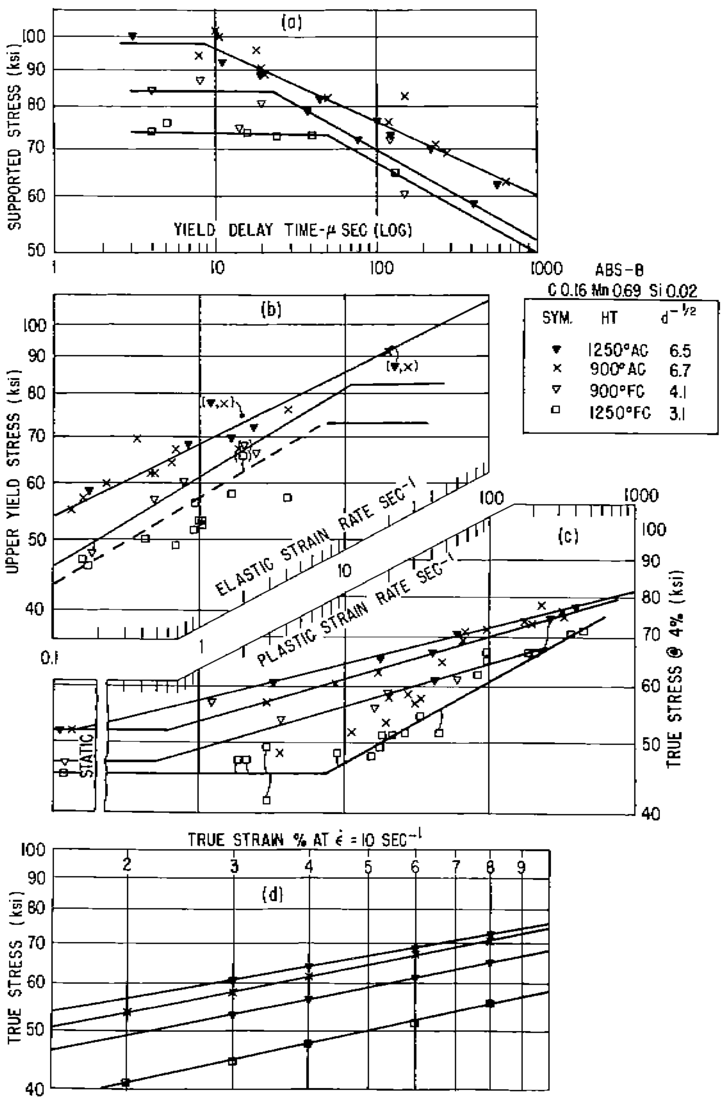

Fig. 7. Summary of dynamic yield and flow data for medium carbon, medium manganese steel, ABS-B.

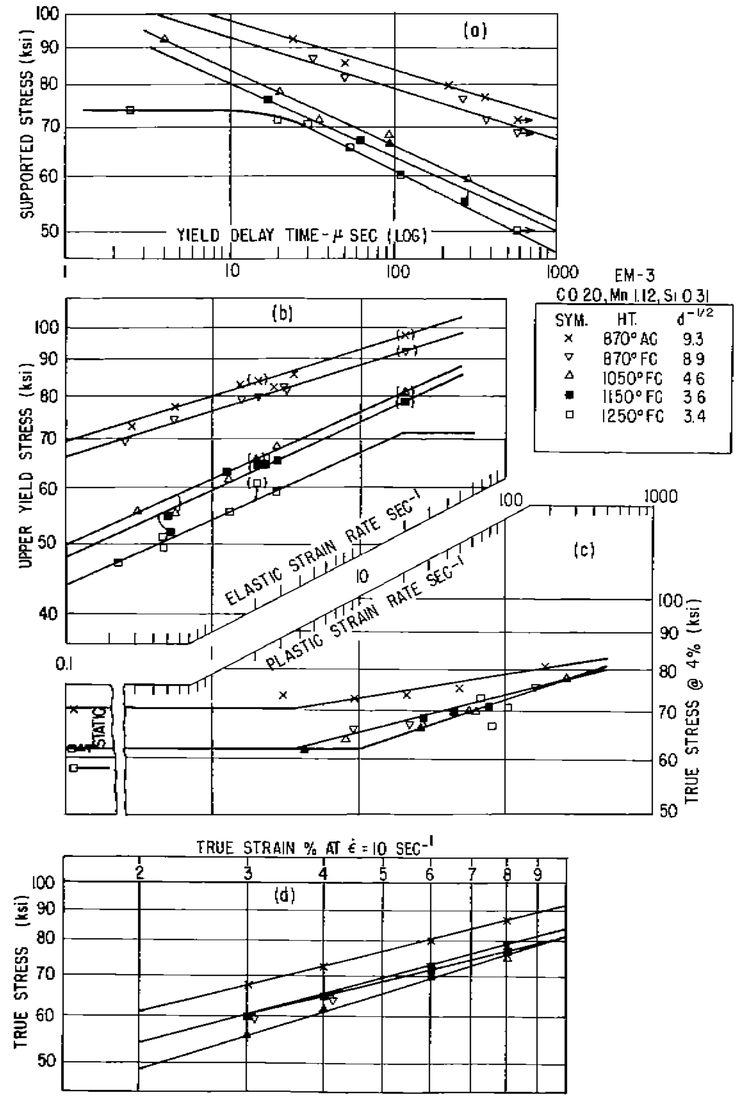

Fig. 8. Summary of dynamic yield and flow data for medium carbon, high manganese steel, EM-3.

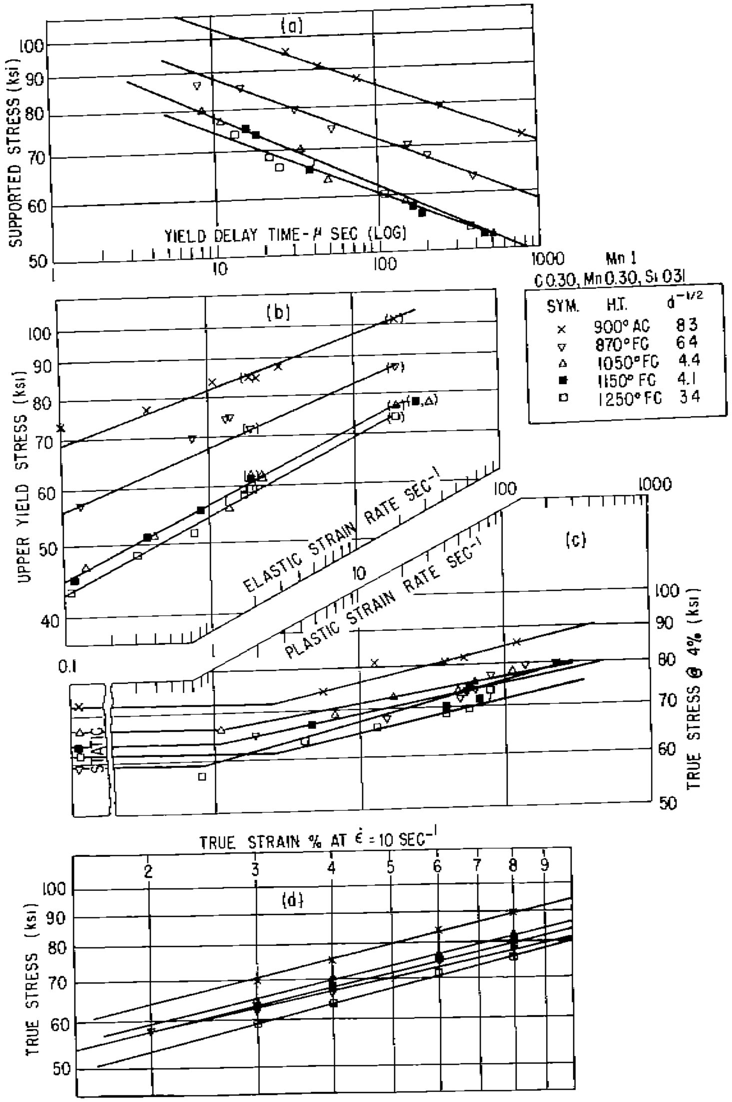

Fig. 9. Summary of dynamic yield and flow data for high carbon, low manganese steel, Mn-1.

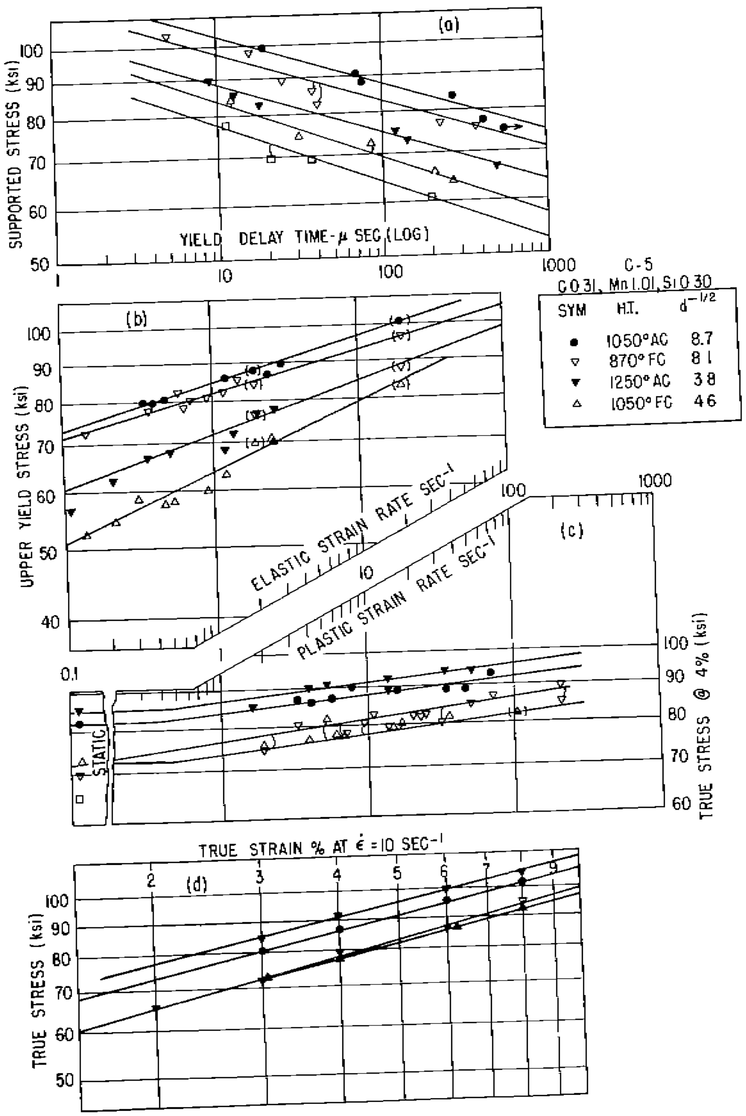

Fig. 10. Summary of dynamic yield and flow data for high carbon, high manganese steel, C-5.

stress vs. strain curves for each test have been picked off at fixed strain levels and plotted vs. instant strain rate on composite curves (not shown). Of this set, values of flow stress at 4% strain, being essentially free from influence of the lower yield effects, are plotted against the applicable instant strain rate in Figs. 3—10, designated (c). The flow strength at any other strain level can be estimated from Figs. 3—10, designated (d). Here the stress vs. strain at a selected strain rate of 10/sec is taken from curves connecting the composite data noted above.

The data summarized in Figs. 3—10 are further condensed for presentation in tabular form. Columns of Table III contain the following information:

Column 1 gives the static lower yield stress.

Columns 2-6 pertain to upper yield or delayed yield effects.

2) 3) and 4) are upper yield stress at elastic strain rates of 0.1, 1.0, and 10.0 per second, respectively. Tendency for some materials, particularly those of large grain size, to reach constant yield stress at very high loading rate (or short delay time) is denoted by brackets on stresses considered to be so affected.

5) $(\sigma_1 - \sigma_{0.1})$, the difference between yield stresses of Col. 3 and Col. 2 is a measure of absolute stress rate sensitivity or the stress increase for a factor of 10 increase in loading rate in the applicable speed range.

6) $(d \log \sigma)/(d \log \dot{\epsilon})$ is the relative measure of loading rate sensitivity, taken as the slope of the logarithmic plot of yield stress vs. strain rate. Since a straight line on such plot will fit the data over an enormous speed range (17) it provides a more generally applicable parameter.

Columns 7-13 pertain to dynamic plastic flow properties.

7) 8) 9) are flow stress σ_f at 4% true strain (corrected from compressive test) for nominal strain rates of 1, 10, and 100 per second respectively.

10) $(\sigma_{f,10.} - \sigma_{f,1.0})$, the difference between flow stresses of Col. 8 and Col. 7, is a measure of absolute sensitivity of flow stress to

TABLE III. DYNAMIC PROPERTIES OF TESTED MATERIALS

Material	1	2	3	4	5	6	7	8	9	10	11	12	13
	Lower Y.S. (ksi) Static	Upper Yield Stress (ksi)/sec 0.1	1	10	$\sigma_1 - \sigma_{.1}$	$\frac{d \log \sigma}{d \log \dot{\epsilon}}$	Flow Stress at 4% ϵ (ksi)/sec 1	10	100	$\sigma_{10} - \sigma_1$	$\frac{d \log \sigma}{d \log \dot{\epsilon}}$	n at 10/sec	θ ksi at 4% ϵ
1010-2													
FC 870 C	27.0	46.6	61.9	76.6	15.3	.093	46.1	53.9	63.0	7.8	.068	.128	120
1050	16.0	36.0	53.0	68**	17.0	.168	40.2	48.5	58.9	8.3	.084	.201	195
1250	19.0	36.0	53.0	63**	17.0	.168	42.0	50.3	60.6	8.3	.080	.164	155
AC 870	31.3	54.9	68.4	85.6	13.5	.098	51.0	57.8	65.4	6.8	.054	.160	174
1050	24.2	46.8	59.2	75.2	12.4	.104	45.2	53.3	62.9	8.1	.072	.169	171
1250	30.6	52.5	64.8	80.1	12.3	.092	54.9	61.4	69.0	6.5	.050	.132	141
1010-1													
FC 870	34.4	62.1	73.3	86.4	11.2	.070	48.7	54.7	61.4	6.0	.050	.222	252
1050	28.0	45.9	57.4	71.7	11.5	.098	48.1	53.3	59.1	5.2	.044	.260	296
1250	25.4	40.3	54.8	68**	14.5	.132	48.7	54.7	61.2	6.0	.050	.248	282
AC 1050	35.6	53.0	63.8	76.4	10.8	.080	55.1	58.3	61.8	3.7	.028	.257	316
1250	30.6*	50.0	60.5	73.2	10.5	.083	59.0	62.2	65.6	3.2	.023	.220	281
1010-4													
FC 870	44.3	62.2	73	86.1	10.9	.071	***	61.3	66.8	--	.038	.252	326
1050	27.5	44.5	55.4	68.9	10.9	.094	"	58.2	65.4	--	.052	.242	294
1150	29.2	46.1	57	70.0	10.9	.088	"	58.2	65.4	--	.052	.258	316
1250	20.4*	44.2	54.2	66.3	10.0	.088	"	55.5	63.4	--	.057	.250	290
AC 870	46.6	62.2	73.1	86.1	10.9	.071	"	65.7	72.3	--	.038	.225	304
Project E													
FC 900	36.9	62.1	76.8	95.4	14.7	.093	55.7	61.5	68.2	5.8	.046	.240	312
950	36.9	60.8	75.3	93.3	14.5	.093	54.3	60.4	67.2	6.1	.046	.250	318
1050	32.6	53.1	68.1	87.0**	15.0	.108	56.6	63.2	70.4	6.6	.047	.238	312
1150	31.8	44.6	63.8	***	19.2	.154	55.7	61.5	68.2	5.8	.046	.247	318
1250	29.2	44.6	63.8	***	19.2	.154	54.3	60.4	67.2	6.1	.046	.248	310
AC 900	44.8	71.0	85.0	102.0	14.0	.093	63.2	70.0	75.2	6.8	.044	.221	308
1250	39.6	62.1	76.8	95.4	14.7	.078	65.0	71.8	79.7	6.8	.044	.192	273
ABS-B													
FC 900	27.2	45.8	60.9	80.0	15.1	.123	--	46.6	--	--	--	.208	236
1250	25.5	43.6	57.2	***	13.6	.120	--	56.0	--	--	--	.221	216
AC 900	38.2	54.1	67.8	85.2	13.7	.098	53.6	61.2	70.0	--	.049	.206	254
1250	33.1	54.1	67.8	85.2	13.7	.098	57.2	64.0	71.8	--	.057	.180	224
EM-3													
FC 870	44.6	66.0	73.3	88.3	10.3	.064	***	65.1	73.2	--	.053	.270	372
1050	33.1	49.8	61.4	76.1	11.6	.092	"	61.4	71.7	--	.065	.250	339
1150	31.8	47.9	59.6	73.7	11.7	.092	"	61.4**	71.7**	--	--	.311	413
1250	28.0*	42.0	54.0	66.8	12.0	.092	"	61.4**	71.7**	--	--	--	--
AC 870	50.4	69.6	80.3	92.8	16.7	.063	"	72.4	78.1	--	.032	.250	381
Mn-1													
FC 870	38.7	55.6	67.4	81.8	11.8	.082	61.2	67.5	71.2	6.3	.052	.228	310
1050	27.0	44.8	56.4	71.1	11.6	.102	64.5	70.0	75.9	5.5	.037	.246	355
1150	26.7	44.8	56.4	71.1	11.6	.102	61.7	67.4	74.1	5.7	.042	.228	315
1250	25.4	42.7	55.1	65**	12.4	.110	***	63.4	70.4	--	.045	.249	330
AC 900	50.9	68.7	81.0	95.6	12.3	.072	***	74.9	83.6	--	.047	.233	361
C-5													
FC 870	50.2	71.3	81.1	92.2	9.8	.054	76.3	81.4	86.7	5.1	.027	.266	441
1050	37.4	51.2	63.1	78.2	11.9	.092	73.4	77.6	82.2	4.2	.025	.250	408
1250	28.0	--	--	--	--	--	--	--	--	--	--	--	--
AC 1050	58.6	73.1	83.9	96.6	10.8	.060	83.3	87.3	91.8	4.0	.022	.242	435
1250	45.8*	60.5	71.1	83.6	10.6	.068	86.2	90.8	95.4	4.6	.021	.236	443

*Proportional Limit
**Extrapolated Value
***Plateau

a factor of 10 change in strain rate in the applicable speed range.

11) $(d \log \sigma_f)/(d \log \dot{\epsilon})$ is the relative measure of flow stress-strain rate sensitivity.

12) n is the strain hardening exponent or slope of the logarithmic plot of true stress vs. true strain (adiabatic). Assuming constant n (for strains less than 10%) the stress-strain curve can be represented by $\bar{\sigma} = K\bar{\delta}^n$, where $\bar{\sigma}$ is true stress, K is a constant and $\bar{\delta}$ is the true strain.

13) θ is the tangent modulus or slope of the nominal compressive stress-strain curve at 4% strain. It can be related to n through the expression

$$\theta = \bar{\sigma}\,(n/\bar{\delta} - 1).$$

The strain hardening exponent n, listed in Table III for each log σ-log ϵ curve (d), permits reconstruction of the stress vs. strain relationship at a 10/sec strain rate. Stress-strain curves at other strain rates may be reconstructed by displacing this curve in graph (d) by a constant stress increment equal to that occurring at the desired strain rate and the 10/sec strain rate shown in graph (c). A characteristic of constant θ or tangent modulus is found in many body-centered cubic metals[16] such as the mild steel employed when temperature rather than strain rate is varied. Thus it is not surprising that this constant θ situation is found to characterize the stress-strain curves resulting from varied strain rate.

DISCUSSION

An important feature of the dynamic behavior of mild steel is the enormous elevation of the upper yield point. Compared to the plastic flow elevation, not only is the rate sensitivity nearly double, but the threshold speed for the appearance of this sensitivity is lower. Since concepts of fracture mechanics also suggest dominance of the yield elevation effect, correlations with fracture behavior might well be attempted with parameters

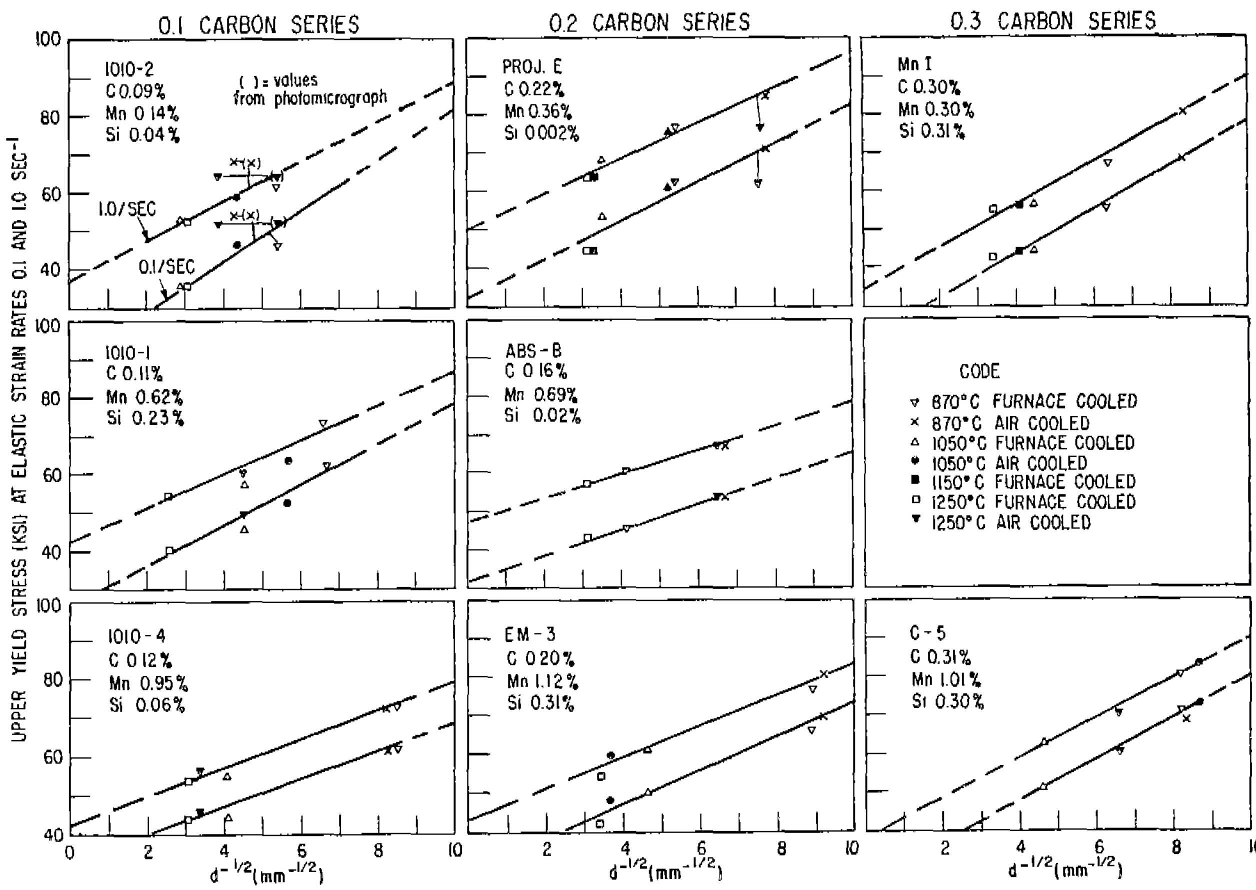

Fig. 11 - Upper yield stress at selected elastic (loading) strain rates of 0.1 and 1.0 per sec against ferrite grain size parameter, $d^{-1/2}$.

related to the upper yield.

The sensitivity of lower yield strength to grain size represented by a plot against $d^{-1/2}$ has been used as a measure of dislocation locking[18] and thus of restraint of plastic flow. The high stresses induced by low temperatures are assumed equivalent to those produced by high strain rates and thus correlated with impact fracture data. With present data, the upper yield stress at selected high loading rates may be plotted directly as shown in Fig. 11. The slopes of these curves, conventionally designated as k, are seen to vary with manganese content at each carbon level.

It will be noted from Fig. 11, as well as from Figs. 3-10 from which it is derived, that the sensitivity of dynamic yield strength to grain size parameter $d^{-1/2}$ tends to decrease with increased rate of loading. In terms of equiva-

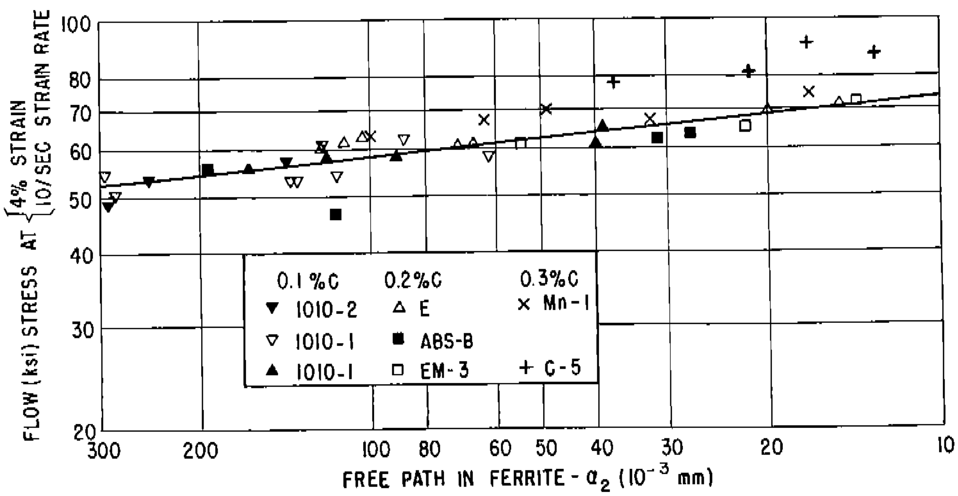

Fig. 12 - Flow stress at selected strain (4%) and strain rate (10/sec) as a function of free ferrite path parameter α_2.

lent temperature decrease, such an effect has been noted by Hahn[19] at temperatures between room and that at which twinning limits the yield strength elevation. Indeed there is every indication that k at very high strain rate would again increase, as the large-grain materials exhibit an early tendency to reach a maximum stress plateau generally associated with the twinning stress limitation.

In a previous publication on delayed yield measurements[16] the present authors noted that dynamic yield strength tended to correlate better with pearlite patch size (at given carbon content) than with either ferrite size parameters. Additional data obtained from this report are inconclusive. Attempts to relate the strengths of all material to ferrite path α_2, as suggested by Gensamer,[20] are reasonably successful (for dynamic flow strength). Thus in Fig. 12 a correlation is found between dynamic flow strength (at $\dot{\epsilon}$ = 10/sec) and the free path between pearlite colonies. The 0.30% carbon steels tend to have significantly higher strengths than the others. However the correlation as a whole is enormously superior to any possible with a simple ferrite grain size parameter.

One effect for which explanation is to be sought is the benefit derived from normalizing or air-cooling mild steel after heating to about 900 C.[21] An indication of abnormally low loading rate sensitivity at a given grain size would suggest a connection to yield properties. While there is a tendency for both

900 C and 1250 C air-cooled steel to exhibit a slightly lower ratio of dynamic to static yield stress, no definite correlation has been established. An effect of fracture toughness rather than yield strength sensitivity variation with normalization is suggested.

CORRELATION WITH FRACTURE PERFORMANCE

Charpy notch bar impact tests have demonstrated satisfactory correlation with service performance in mild ship plate if comparison is made at a low energy level. Although a sharper notch would be preferred, the test at low energy levels provides conditions not impossible of a fracture mechanics evaluation. Thus attempts to correlate present results with available Charpy data provide a reasonable basis for comparison. Accepting a 15 ft-lb Charpy energy as sufficiently brittle, the work of Rinebolt and Harris[22] provides an empirical basis for rating effects of compositional variables. On a series of steels similar to these, addition of one per cent by weight carbon was found to increase the 15 ft-lb transition temperature by 500 F;* silicon by 125 F; and manganese to decrease by 100 F. The sensitivity of upper yield stress to grain size or k appears to bear a correlation with shift in the transition temperature predicted from this rule as shown in Fig. 13. At an elastic strain rate of 0.10/sec a single curve can be fitted through all points of the medium (0.20%) and high (0.30%) carbon steels; another curve connects the low (0.10%) carbon steels. These two curves can be brought closer together by selecting a higher level of loading rate for comparison, shown by way of example here for elastic loading strain rate 1.0/sec.

Success in associating a measure of grain size sensitivity with fracture performance has interesting implications. Consider the general shape of

---

*More recent data (unpublished) suggests a somewhat reduced sensitivity to carbon content (e.g. 200 F 1% C). Use of such a factor would significantly improve the correlation between 0.10% C and higher carbon steels in Fig. 13.

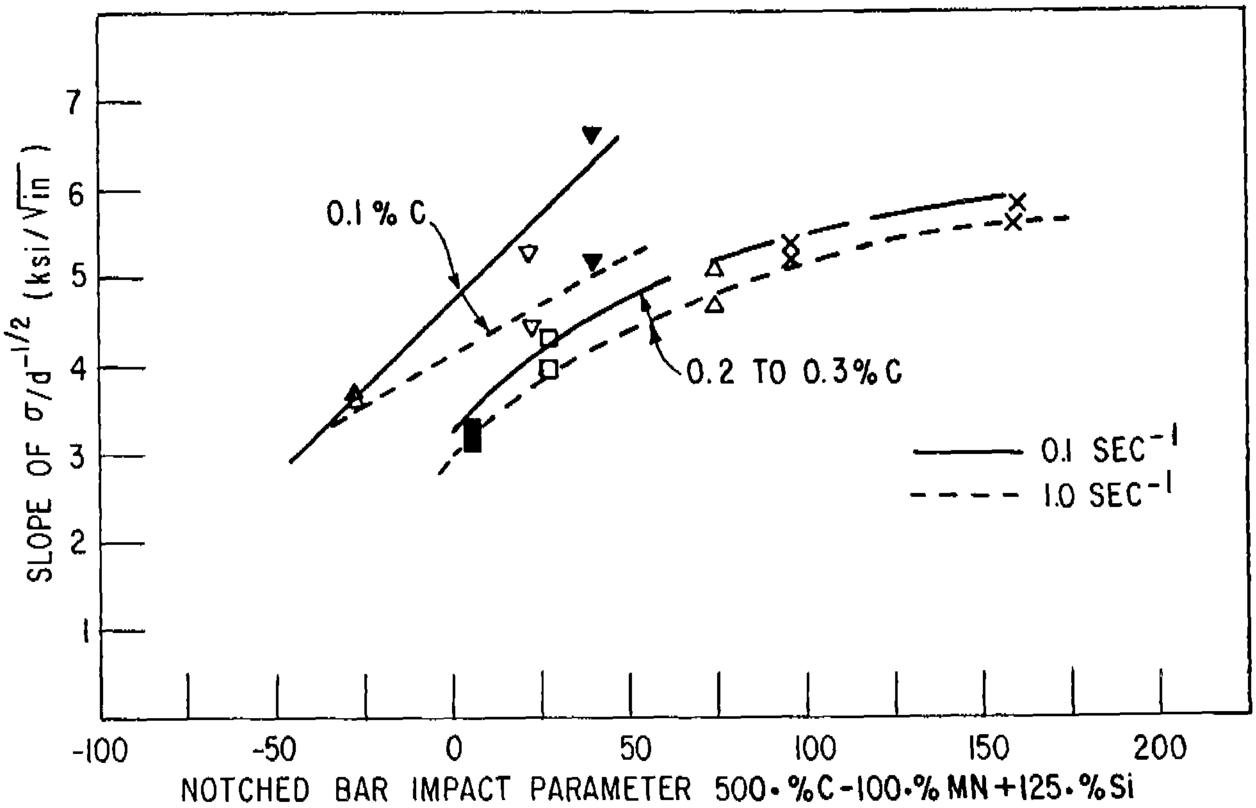

Fig. 13 - Comparison of sensitivity of yield stress to grain size to a notched bar transition temperature parameter based on effects of composition.

the curves (Fig. 13). For materials with compositions giving a low transition temperature expectancy, the influence of the parameter k appears much stronger than for high temperature. Thus for the high carbon and/or silicon steels, large changes in transition temperature appear to occur essentially independent of variation in k. This would suggest that some other factor, perhaps a change in fracture toughness rather than in yield strength parameters, is operative to alter the fracture brittleness characteristics in this range. It is generally true that the more highly alloyed steels, having also greater static yield strength, tend to exhibit reduced relative sensitivity of yield stress to loading rate (Table III Col. 6). Only the absolute sensitivity tends to remain constant with varied static yield strength level (Table II, Col. 5). Since the Irwin fracture mechanics[5] successfully dimensions the plastic zone size as a function of a ratio rather than the difference between fracture stress parameter and yield stress parameter, a measure of the relative rather than the absolute yield strength enhancement due to rapid strain rate should be applicable.

The failure to merge correlations of low carbon with medium and high carbon levels in Fig. 13 is suggestive of cause related to the substantial differences in mode transition behavior between these composition levels. Low carbon steels exhibit change from fully brittle to fully ductile most abruptly with temperature rise, the higher carbon increasingly more gradual. Mailänder[2] has shown a sensitivity to impact velocity much greater for low carbon steel than for high. If this is so, then the sensitivity of transition temperature to carbon additions should be a function of impact velocity. The increase in transition temperature per unit carbon addition might thus be expected to be reduced at low carbon levels if greater impact velocity were employed. Such a change would tend to draw closer together the transition temperatures of 0.10 and 0.20% carbon steels, thus providing better correlation between the parameter k and the transition temperature parameter.

There are general effects of varied carbon and manganese level discernable in the data which are qualitatively consistent with impact fracture behavior. In general both relative and absolute upper yield point rate sensitivity at comparable grain size decrease with increasing manganese, an effect reasonably associated with corresponding improvement in fracture mode transition temperature. This effect diminishes at higher carbon levels, consistent with the leveling of the grain size parameter (Fig. 11). Greater sensitivities are also evident in the larger grain material, consistent with their greater brittleness.

The strain hardening exponent, n, may be taken as an indication of the extensional strain at tensile instability. As such it should influence the extent of plastic deformation near the free surfaces of a plate in fracture. It is of interest here to note that at a given carbon level there is a tendency for n values to increase with increased manganese content in agreement with this concept.

While study of plastic flow properties can provide bases for understanding of an important part of the fracture process, its limitations are basic. A description of fracture in terms of two parameters, a fracture toughness stress parameter, and a yield strength parameter, is essential to our present state of knowledge. This is not to preclude an eventual explanation of both as consequences of a single basic process, as for example one describable by dislocation mechanics. However, pending this it is helpful to think of these as independent material properties. Fracture performance can be affected by either. A study of one can indicate only effects of one.

Fracture initiation and propagation are extremely sensitive to flaws and to the size and geometry of the structure. The plastic flow test, on the other hand, is rather insensitive to these variables. Thus changes in fracture performance introduced by these variables cannot be directly associated with flow properties except as they may be used in a proper analysis of the mechanics of the situation.

CONCLUSIONS

If dislocation locking is evaluated as the sensitivity of upper yield stress to grain size ($d^{-1/2}$) at sufficiently high loading rates, a correlation is found to exist between it and the expected variations in Charpy impact transition temperature owing to composition variables carbon, manganese and silicon. It might thus be inferred that additions of these elements, through their effect on dislocation movement, influence fracture brittle tendencies largely through variation in the yield stress, and not primarily through changes in fracture toughness. At higher carbon levels changes in transition temperature are not explicable on this basis and here dominance of the fracture toughness or possibly simply the general rise in nonrate sensitive yield strength are suggested.

ACKNOWLEDGMENTS

The authors are particularly grateful to Dr. G. R. Irwin, Superintendent of the Mechanics Division, and Mr. J. A. Kies, Ballistics Branch Head, for their interest and cooperation. Data collection and processing were assisted by K. Coxe and J. Stinson. The support of the Ship Structure Committee provided continued incentive supplementing basic support of this project from Research Navy Funds.

REFERENCES

1. Manjoine, M. J., "Influence of Rate of Strain and Temperature on Yield Stresses of Mild Steel," Journal of Applied Mechanics, vol. 11, p. A211 (1944).

2. Mailänder, R., "Verhaltnis der Ergebnisse von Statischen und Dynamischen Kerbbiegeversuchen Zueinander," Arch. f. Eisen, vol. 10, p. 109 (1936).

3. Hall, W. J., Mosborg, R. J., and McDonald, V. J., "Brittle Fracture Propagation in Wide Steel Plates," The Welding Journal, 36:1, Research Supplement, 1s-8s (1957).

4. Ludwik, P., Elemente der Technologischen Mechanik. Berlin: 1909.

5. Irwin, G. R., Fracture Testing of High-Strength Sheet Materials Under Conditions Appropriate for Stress Analysis (U. S. Naval Research Laboratory Report 5486), July 27, 1960.
   or
   Irwin, G. R., "Plastic Zone Near a Crack and Fracture Toughness," Proc. of the Seventh Sagamore Ordnance Materials Research Conference, Raquette Lake, N. Y., August 1960.

6. Srawley, J. E., "Fracture Appearance of High Strength Steels and Other Alloys," Proc. of the Seventh Sagamore Ordnance Materials Research Conference, Raquette Lake, N. Y., August 1960.

7. Demer, L. J., A Review of Observations on the Cracking Characteristics and Fractures of Laboratory Fatigue Specimens (WADC Tech. Note 55-527), Sept. 1955.

8. Steigerwald, E. A., "Delayed Failure of High Strength Steel in Liquid Environments," Trans. ASM, to be published.

9. Rostaker, W., Embrittlement by Liquid Metals. New York City· Rinehold Publishing Co., 1960.

10. Owen, W. S., Whitmore, D. H., Sullivan, C. P., Averbach, B. L., and Cohen, M., The Relationship of Microstructures to the Charpy Impact and Low Temperature Tensile Properties of Two Ship Steels (Ship Structure Committee Report Serial No. SSC-102). Washington: National Academy of Sciences-National Research Council, June 18, 1956.

11. Ripperger, E. A., Stress-Strain Characteristics of Materials at High Strain Rates, Part V, "Dynamic Compressive Yield Stresses," (Sandia Corp. Contract AT(29-2)-621). Austin. Univ. of Texas, August 1960.

12. Krafft, J. M., "Critical Comparison of Moving Bar Impact with Gas Expansion Machines for Dynamic Loading of Metals," Jour. Appl. Polymer Sci., to be published.

13. Krafft, J. M., "Instrumentation for High-Speed Strain Measurement," Response of Metals to High Velocity Deformation. New York· Metallurgical Society Conferences, Interscience.

14. Krafft, J. M., An Interpretation of Lower Yield Point Plastic Flow in the Dynamic Testing of Mild Steel (Ship Structure Committee Report Serial No. SSC-123). Washington. National Academy of Sciences-National Research Council, June 26, 1961.

15. Vigness, I., Krafft, J. M., and Smith, R. C., "Effect of Loading History upon the Yield Strength of a Plain Carbon Steel," Proc. Conf. on the Properties of Materials at High Rates of Strain. London. Inst. Mech. Eng., p. 139, 1957.

16. Beeukes, R., Jr., "Plasticity and Fracture," Proc. of the Third Sagamore Ordnance Materials Research Conference. Durham, N. C.: Duke Univ., December 1956.

17. Krafft, J. M. and Sullivan, A. M., "Effect of Grain Size and Carbon Content on the Yield Delay-Time of Mild Steel," Trans. ASM, vol. 51, p. 643 (1959).

18. Heslop, J. and Petch, N. J., "Dislocation Locking and Fracture in α-Iron," Phil. Mag., vol. II (Eighth Series), p. 649 (1957).

19. Hahn, G. T., Private communication.

20. Gensamer, M., "Strength and Ductility," (Campbell Memorial Lecture), Trans. ASM, vol. 36, p. 30 (1946).

21. Frazier, R. H., Boulger, F. W., and Lorig, C. H., "Influence of Heat Treatment on the Ductile-Brittle Transition Temperature of Semikilled Steel Plate," Trans. AIME, vol. 203, p. 323 (1955).

22. Rinebolt, J. A., and Harris, W. J., Jr., "Effect of Alloying Elements on Notch Toughness of Pearlitic Steels," Trans. ASM, vol. 43, p. 1175 (1951).

COMMITTEE ON SHIP STEEL

Chairman:

Professor John Chipman
Head, Department of Metallurgy
Massachusetts Institute of Technology

Vice Chairman:

Mr. M. W. Lightner
Vice President, Research and Technology Division
United States Steel Corporation

Members:

Professor C. S. Barrett
Institute for the Study of Metals
University of Chicago

Professor D. K. Felbeck
Department of Mechanical Engineering
University of Michigan

Mr. Paul Ffield
Assistant Manager of Research
Bethlehem Steel Company

Professor Maxwell Gensamer
Professor of Metallurgy
School of Mines
Columbia University

Dr. J. R. Low, Jr.
Metallurgy Research Unit
Research Laboratory, General Electric Company

Mr. T. S. Washburn
Manager, Quality Control Department
Inland Steel Company

Mr. T. T. Watson
Director of Research
Lukens Steel Company